CLINICAL SCIENCE

Pathological and ultrastructural analysis of surgical lung biopsies in patients with swine-origin influenza type A/H1N1 and acute respiratory failure

Vera Luiza Capelozzi,[I] Edwin Roger Parra,[I] Manoel Ximenes,[II] Ricardo Helbert Bammann,[III] Carmen Silvia Valente Barbas,[IV] Marid Irmd Seixas Duarte[V]

[I]Pathology - Faculdade de Medicina da Universidade de São Paulo, São Paulo, SP, Brazil. [II]Thoracic Surgery Unit- Hospital de Base do Distrito Federal - Brasilia, Brazil. [III]Thoracic Surgery- Instituto de Infectologia Emílio Ribas - São Paulo, SP, Brazil. [IV]Intensive Care Unity- Hospital Israelita Albert Einstein -, São Paulo, SP, Brazil. [V]Anatomy- Hospital das Clinicas da faculdade de Medicina da Universidade de São Paulo, Sao Paulo, SP, Brazil.

BACKGROUND: Cases of H1N1 and other pulmonary infections evolve to acute respiratory failure and death when co-infections or lung injury predominate over the immune response, thus requiring early diagnosis to improve treatment.

OBJECTIVE: To perform a detailed histopathological analysis of the open lung biopsy specimens from five patients with ARDS with confirmed H1N1.

METHODS: Lung specimens underwent microbiologic analysis, and examination by optical and electron microscopy. Immunophenotyping was used to characterize macrophages, natural killer, T and B cells, and expression of cytokines and iNOS.

RESULTS: The pathological features observed were necrotizing bronchiolitis, diffuse alveolar damage, alveolar hemorrhage and abnormal immune response. Ultrastructural analysis showed viral-like particles in all cases.

CONCLUSIONS: Viral-like particles can be successfully demonstrated in lung tissue by ultrastructural examination, without confirmation of the virus by RT-PCR on nasopharyngeal aspirates. Bronchioles and epithelium, rather than endothelium, are probably the primary target of infection, and diffuse alveolar damage the consequence of the effect of airways obliteration and dysfunction on innate immunity, suggesting that treatment should be focused on epithelial repair.

KEYWORDS: Open lung biopsy; Acute lung injury; Diffuse alveolar damage; Virus; Electron microscopy; Innate immunity.

Capelozzi VL, Parra ER, XimenesM, Bammann RH, Barbas SV, Duarte MIS. Pathological and ultrastructural analysis of surgical lung biopsies in patients with swine-origin influenza type A/H1N1 and acute respiratory failure. Clinics. 2010;65(12):1229-1237.

Received for publication on July 7, 2010; **First review completed on** August 2, 2010; **Accepted for publication on** September 7, 2010

E-mail: erparra2003@yahoo.com.br

Tel.: 55 11 3826-1422

INTRODUCTION

Recently, a novel swine-origin influenza A (H1N1) virus with molecular features of North American and Eurasian swine, avian, and human influenza viruses[1-4] has been associated with an outbreak of respiratory disease. According to the World Health Organization (WHO), between 25 April and 11 October 2009, 399,232 confirmed cases of H1N1 influenza virus and 4,735 deaths occurred throughout the world.[5] Brazil reported 1,528 deaths up to 10 November 2009.[6]

Swine-origin influenza A (H1N1) virus infection can cause severe acute respiratory failure (ARF), requiring admission to an intensive care unit (ICU) in 15–30% of previously healthy young to middle-aged people.[3,4,7,8] Death may occur when co-infections or lung injury prevail over the immune response, resulting in a progressive worsening of lung function (low compliance and oxygenation). Early diagnosis and a complete understanding of the pathological features of the H1N1 virus are important to help to improve treatment and the prognosis of this lethal disease. Analysis of the lung tissue from an open lung biopsy (OLB) of these severe cases can help in understanding the pathogenesis of this severe and sometimes fatal development. Until now, no reports of OLB findings used to guide the treatment of patients with H1N1 pneumonitis have been published, although according to many authors OLB is safe and diagnostically useful in patients with ARF, enabling appropriate therapy.[9-12]

The pathogenesis of ARF associated with swine-origin influenza virus (S-OIV) infection in humans is unknown. The influenza virus triggers pulmonary inflammation owing to an infiltration of inflammatory cells and an immune response. Bronchial epithelial cells are the primary target and the principal host for the virus.[13,14] Normally, influenza viruses are recognized and destroyed by innate immune mechanisms which involve macrophages, interferon (IFN) α, β and other cytokines, natural killer (NK) cells and complement. When influenza viruses escape from these early defense mechanisms, they are captured and eliminated by adaptive immune mechanisms, where T and B cells and their antigen-specific effectors (cytotoxic T lymphocytes, cytokines such as IFNγ and antibodies) target the virus. Additionally, antigen-specific memory cells (T and B cells) are involved in the prevention of the subsequent viral infection.[14]

Thus, pathological findings obtained by an OLB, coupled to ultrastructural and immunologic analysis, may have an impact on decisions about changes in treatment strategies employed for these critically ill patients, and also provide a greater understanding of the pathophysiology of S-OIV infection. The objective of this study was to analyze pathologically and ultrastructurally S-OIV lung infection and the pulmonary immune response in a series of five cases with OLB.

METHODS

Patients and Collection of Specimens

We studied pathologically and ultrastructurally five patients suspected of having a pandemic S-OIV virus who developed ARF requiring ventilatory support. Nasal swabs for RT-PCR for H1N1 were collected from all patients. The OLBs indicated by the clinicians were carried out after receiving consent from the families. These patients had a severe evolution of the virus and more information about the physiopathology of the disease was required in order to provide adequate treatment. If no improvement of the respiratory status was seen in the patients with ARF after ≥5 days (defined as no decrease of the Lung Injury Score) an OLB was indicated.[15]

Lung tissue sections (4 μm thick), prepared from 10% formalin-fixed, routinely processed, paraffin-embedded blocks, were stained with hematoxylin-eosin. The following methods of histochemical staining were carried out: Grocott's methenamine silver stain, Brown–Brenn, and Ziehl–Neelsen. The following pathological changes were analyzed: a) necrotizing bronchiolitis, b) alveolar collapse, c) dilatation of the airspaces, d) hyaline membrane, e) fibroplasia, f) squamous metaplasia, g) multinucleated cells, h) alveolar hemorrhage, i) acute inflammatory exudates, j) atypical pneumocytes. Pathological changes were graded, using two sections, according to a five-point semiquantitative severity-based scoring system as: 0 = normal lung parenchyma, 1 = changes in 1–25%, 2 = changes in 26–50%, 3 = changes in 51–75%, and 4 = changes in 76–100% of examined tissue. This semiquantitative analysis is currently routinely used in most studies of the department of pathology of the University of São Paulo Medical School.[16,17]

For immunohistochemistry, the avidin–biotin–peroxidase complex and streptavidin–biotin enzyme complex immunostaining methods were used with antibodies against: lymphocytes CD4 (clone: MO834, dilution 1:1000), CD8 (clone: M7103, dilution 120), CD20 (clone: M755, dilution 140), macrophages-histiocytes CD68 (clone: M814, dilution 130), mouse monoclonal antibodies from DAKO, Carpinteria, CA, USA; S100 (clone: Z311, dilution 11000) rabbit polyclonal antibodies from DAKO; CD1a (clone: MCA1657, dilution 1: 200) mouse monoclonal antibodies from Serotec, Oxford, UK; natural killer, NK (clone: MS136P, dilution 11000) mouse monoclonal antibodies from Neomarkers, Fremont, CA, USA; interleukin 4 (IL-4) (dilution 140), IL-10 (dilution 140) goat polyclonal antibodies from R&D Systems, Minneapolis, MN, USA; IFNγ (clone: MAB285, dilution 130), mouse monoclonal antibodies from R&D Systems; tumor necrosis factor alpha (TNFα) (clone: AF210NA, dilution 140) all mouse monoclonal antibodies from R&D Systems; inducible nitric oxide synthase (iNOS) (dilution 1500) polyclonal rabbit from Calbiochem, La Jolla, CA, USA.

Immunohistochemical reactions were carried out in accordance with the manufacturer's instruction. Diaminobenzidine was used as the color substrate, and Meyer's hematoxylin was used for counterstaining. Cell immunophenotypes and immune expression of cells using the different methods of immunohistochemical staining were identified and graded according to a five-point semiquantitative intensity-based scoring system as: 0 = negative, 1 = positive in 1–25%, 2 = positive in 26–50%, 3 = positive in 51–75%, and 4 = positive in 76–100% of examined tissue.[18]

Small blocks (1 mm^3) of lungs were fixed in 2% glutaraldehyde/2% paraformaldehyde in cacodylate buffer overnight, then fixed in 1% osmium tetroxide, dehydrated, and embedded in araldite. Ultrathin sections obtained from selected areas were double-stained and examined in a Philips TECNAI 10 electron microscope at 80 kV. For each electron microscopy image (15/case), the following structural changes were analyzed: a) cytoplasmic swelling, b) degenerative changes, c) sloughing of necrotizing alveolar epithelial cell type I (AECI) and II (AECII), d) denudation of the epithelial basement membrane, e) hyaline membranes, f) alveolar septal collapse, g) viral particles such as tubuloreticular structures (TRS) and cylindrical confronting cisternae (CCC), h) multinucleated AECII. Ultrastructural findings were graded according to a five-point semiquantitative severity-based scoring system as: 0 = normal lung parenchyma, 1 = changes in 1–25%, 2 = changes in 26–50%, 3 = changes in 51–75%, and 4 = changes in 76–100% of examined tissue.[16,17]

RESULTS

Patients

Five patients (two male, three female) mean age 48 years (range 35–81) were studied; only patient No 4 had preexisting medical illnesses (Table 1) and chest x-ray abnormality at disease onset. All the patients presented with a 4–10 days' (median 5 days) history of shortness of breath and flu-like symptoms and rapid clinical deterioration. They were transferred to the ICU for tracheal intubation and ventilation (range 8–25 days; median 17) and diagnosed as having ARF.[15] All the patients received 75 mg twice a day by nasal enteral tube of olsetamivir (range 4–14 days; median 10) and intravenous steroids (range 9–20 days; median 12). After obtaining these results the dose was changed from 75 mg twice a day to 150 mg twice a day through a nasal enteral tube, in accordance with the

Table 1 - Clinical features of the patients.

	Patients				
	Case 1	Case 2	Case 3#	Case 4	Case 5
Age	35	35	39	81	51
Sex	Male	Female	Female	Female	Male
Premorbid disease	Absent	Absent	Absent	RA	Absent
Illness (days*)	4	7	5	5	10
Oseltamivir (days*)	10	14	10	4	4
Steroids (days*)	10	9	16	12	20
Intubation (days*)	10	8	25	17	20
Status	Alive	Alive	Dead	Alive	Dead
NPA	+	+	+	+	+
Lung biopsy	+	+	+	+	+
Lung EM	+	+	+	+	+

*Duration of illness or treatment.
#Pregnant.
EM, electron microscopy for SALI associated with influenza A; NPA, nasopharyngeal aspirate; RA, rheumatoid arthritis.

Brazilian guidelines. The presence of the H1N1 virus was confirmed in all five patients (Table 1) by nasal swab or lung tissue positivity of RT-PCR according to guidelines from the Centers for Disease Control and Prevention.[19] Other microbiological investigations, including the isolation of other viruses, were negative. During the evolution of disease in the patients in the ICU, *Staphylococcus aureus* was isolated from a blood culture (patients 2 and 3) and *Klebsiella* spp were identified in tracheal aspirate specimens (patient 1). Patients 1, 2 and 4 are alive, but patients 3 and 5 died of respiratory failure, with concurrent congestive heart failure, hepatic encephalopathy, and acute renal failure.

Necrotizing Bronchiolitis, Collapsogenic Diffuse Alveolar Damage and Alveolar Hemorrhage

Figure 1 depicts the pathological findings in the surgical lung biopsy specimens. The main pathological features were necrotizing bronchiolitis, clastogenic diffuse alveolar damage (DAD), and alveolar hemorrhage (Table 2). Pulmonary specimens from patients 3 and 5 presented more intense changes at optical microscopy. The membranous and respiratory bronchioles were extensively compromised by epithelial necrosis, squamous metaplasia, and obliteration by fibroplasia (Figure 1A–F). The parenchyma was modified by extensive alveolar collapse, dilatation of the airspaces, alveolar hemorrhage, and sparse hyaline membrane formation (Figure 1G–I). There was interstitial thickening, with mild to moderate fibroplasia (Figure 1I), but a disproportionately sparse infiltrate of inflammatory cells, mainly histiocytes, including multinucleated forms, lymphocytes and megakaryocytes (Figure 1J–K).

Atypical bronchiolar and alveolar epithelial cells (AECs) were seen in all five patients, although the distribution was focal (Figure 1J). These atypical forms included multinucleated giant cells with irregularly distributed nuclei (Figure 1K, L) or bronchiolar and AECs with large atypical nuclei, prominent eosinophilic nucleoli, and granular amphophilic cytoplasm (Figure 1M). However, distinct viral inclusions were not apparent.

Bronchial and Alveolar Epithelium Necrosis and Viral-like Particles

The ultrastructural features were represented by bronchial and alveolar epithelium necrosis, a destroyed alveolar epithelium/basement membrane unity and the presence of viral-like particles (Table 3). Patients 3 and 5 presented more prominent changes at submicroscopic level. Cytoplasmic swelling, necrosis, and degenerative changes of the endoplasmic reticulum and other organelles were present in bronchial and AECs (Figure 2A–C). A large number of bronchiolar and AECs were detached from the basement membrane and were showing apoptosis (Figure 2A, B). Lymphocytes also exhibited apoptosis. Sloughing of apoptotic bronchiolar cells and AECs causing denudation of the epithelial basement membrane was followed by deposition of hyaline membranes (Figure 2D).

Ultrastructural evidence of alveolar collapse was also present by the apposition of the alveolar septa (Figure 2E–G). The regenerating bronchiolar epithelium extended along the adjacent alveolar septa showing features of cells with prominent surface microvilli with decreased or absent lamellar bodies and considerable cytologic atypia (Figure 2H–L). Increased myofibroblasts and collagen fibers were also present (Figure 2I). Multinucleated epithelial cells with prominent nucleoli were noted in most cases, although such cells were sparse (Figure 2K). The proliferating bronchiolar and AECs containing TRS and CCC, probably representing residual viral-like particles, were distinguished in all cases (Figure 2M–R). TRS appeared as reticular aggregates of branching membranous tubules located within the cisternae of the endoplasmic reticulum (Figure 2M–O) or were compact (Figure 2Q, R). CCC were identified as elongated, slightly curved cylindrical structures (Figure 2P, Q), ring shaped (Figure 2R) or fused membranous lamellae, representing cisternae of endoplasmic reticulum.

Deficient Innate and Adaptative Immune Response

Figure 3 depicts immunological findings in the surgical lung biopsy specimens. The immunologic features were dominated by a decrease in the innate and adaptive immune response (Table 4). Patients 3 and 5 presented with immunologic impairment.

In all patients small aggregates of macrophages, CD4+ T-helper cells, CD8+ T-cytotoxic cells, CD20+ B-cells, CD1a+ dendritic cells, S100+ dendritic cells, natural killer lymphocytes were present around vessels and bronchioles. Dendritic cells and TNFα were expressed sparsely in macrophages, AECs and endothelial cells, whereas IFNγ was expressed in small mononucleated cells in lungs from patients with S-OIV. There was a very strong expression of IL-4, IL-10 and iNOS in small mononucleated cells.

DISCUSSION

This case series documents for the first time the pathological and ultrastructural findings of lung tissue from five patients admitted to the ICU with ARF and S-OIV infection who were submitted to OLB.

S-OIV (H1N1) virus and the pulmonary syndrome is an acute respiratory illness, first identified in Mexico with at present, 399,232 cases registered, 4,735 deaths, affecting more than 179 countries.[2,5] Our patients, most of them previously healthy, had an atypical influenza-like illness that progressed during a period of 5–7 days.

The two patients who died showed a higher degree of pathological commitment of the disease at the OLB. Most of our patients were young to middle-aged and had previously been healthy. Increased risk for severe S-OIV illness is found

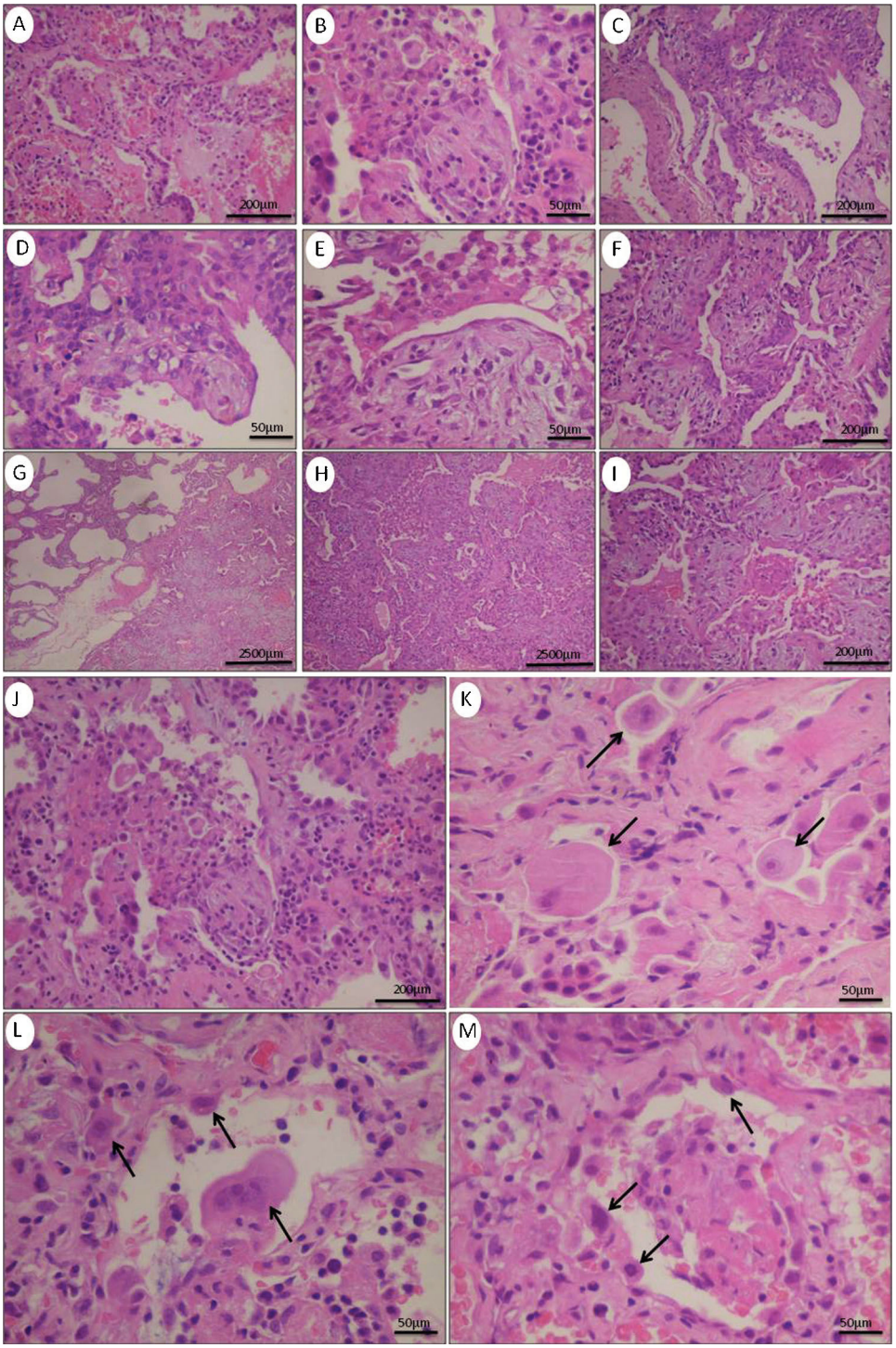

Figure 1 - Lung sections from N1H1 patients examined by Hematoxilyn Eosin staining. This panel show pulmonary parenchyma modified by extensive alveolar lesion characterized by alveolar hemorrhage (A), disproportionately sparse infiltrate of inflammatory cells (B) and collapse alveolar areas with dilatation of the airspaces (C). In other areas show diffuse alveolar damage with interstitial thickening (D), mild to moderate fibroplasia (E), hyaline membrane formation (F) and intra-alveolar fibrin exudates (G to I). Intra-alveolar fibrin exudates similar with moderate infiltrate of inflammatory cells characterized by histiocytes, lymphocytes, megakariocytes and multinucleated forms (J). These atypical forms included multinucleated giant cells with granular amphophilic cytoplasm, irregular, large and atypical nuclei and prominent eosinophilic nucleoli (arrows) (K to M), (Hematoxilyn Eosin).

in young children, 10–19 age groups, patients older than 65 years, pregnant women, obese people and those with comorbidities.[1,7,20] Fifteen to thirty per cent of patients with H1N1 infection required ICU admission. Mortality among the patients who required mechanical ventilation was around 58%.[7]

In our case series the OLB findings showed that the lung damage was most likely due to infection by the influenza

Table 2 - Semiquantitative analysis of pulmonary pathological features of patients with severe acute lung injury.

	Patients				
	Case 1	Case 2	Case 3	Case 4	Case 5
Necrotizing bronchiolitis	3 (4–4)	2.5 (2–3)	3.5 (3–4)	2.5 (2–3)	4 (4–4)
Alveolar collapse	3 (2–4)	3 (3–3)	3.5 (3–4)	2 (1–3)	4 (4–4)
Dilatation of the airspaces	3 (2–4)	2.5 (2–3)	3 (2–4)	2.5 (2–3)	2 (1–3)
Hyaline membrane	1.5 (1–2)	2 (2–2)	1.5 (1–2)	2 (1–2)	2 (1–3)
Alveolar hemorrhage	3 (2–4)	3 (3–3)	3.5 (3–4)	2 (1–3)	4 (4–4)
Fibroplasia	2 (1–3)	2 (2–2)	2 (1–3)	2 (1–3)	1 (1–1)
Squamous metaplasia	2 (1–3)	1 (1–1)	3 (2–4)	1 (1–1)	0 (0–0)
Multinucleated forms	2 (1–3)	1 (0–2)	2.5 (2–3)	2 (1–3)	2 (1–3)
Acute inflammatory exudates	1.5 (1–2)	1.5 (1–2)	1 (1–1)	2 (1–3)	3 (2–4)
Atypical pneumocytes	2 (1–3)	1.5 (1–2)	2 (2–2)	1 (0–2)	2 (2–4)

The lung tissue score was obtained independently by two different investigators. The pathologic findings were graded according to a five-point semiquantitative severity-based scoring system: 0 = normal lung parenchyma; 1 = changes in 1–25%; 2 = 26–50%; 3 = 51–75%; and 4 = 76–100% of the examined tissue.

virus. The main pathological finding revealed necrotizing bronchiolitis and DAD, respiratory epithelial cells probably being the primary target of the infection. The extensive destruction of the respiratory and AECs and dysfunction in the immune and adaptative immune response led to DAD. As previously reported, possible mechanisms of damage include direct injury to the respiratory and alveolar epithelium exposing the basement membrane and leading to alveolar collapse by loss of surfactant,[13,14,21] with a secondary cytokine storm.[22] This is followed by exudation of macromolecules from the circulation, which finally form hyaline membranes. Activation of the cytokines is part of the immune reaction aiming to eradicate the virus. In this study, the systemic IFNγ and TNFα cytokine activation probably resulted in reactive hemophagocytic syndrome in the bronchiole-associated lymphoid tissue and possibly also mediated the epithelial necrosis.[23] A mild inflammatory infiltration is most often seen in viral pneumonias; this has been explained by a cytokine-mediated blockade of lymphocytopoiesis and also by blockade of release from the bone marrow.[24]

In our cases, expression in the lung of IFNγ by small mononucleated cells and TNFα by macrophages and AECs was low. This finding may be supported by Kim and colleagues,[25] who described in S-OIV infection, maximal indices of TNFα expression in lungs of infected pigs in the first days of the infection and then a gradual decrease. Conversely, we found a very strong expression of IL-4, IL-10 and iNOS by macrophages. The sparse inflammatory and immune reaction found in our samples, which involves targetting of the virus by NK cells, lymphocytes T and B cells, CD8+ cytotoxic T-lymphocyte cells, as well as CD1a and S100 cells, may be due to a combination of lymphoid tissue necrosis and apoptosis and exhaustion of lymphoid proliferation in response to the cytokine overdrive. In addition, the high IL-10 expression associated with its anti-inflammatory action may explain the low degree of inflammation observed in our cases. Taken together, our results suggest that in S-OIV infection, altered innate and adaptative immune responses may lead to incomplete virus eradication in the primary target of the infection and, consequently, imbalance between inflammation and reparation, resulting in bronchiolar obliteration and DAD.

DAD is likely to be a consequence of bronchiolar obstruction and consequent hypoxia rather than direct invasion of the viruses. It is a severe pattern of lung injury and could be secondary to various pulmonary and extrapulmonary insults.[26] In this series of cases we found DAD in which alveolar collapse was prominent, differing from classic DAD found in ARF or secondary to other pulmonary and extrapulmonary insults. This finding may have important implications in the ventilation strategy of the patients.[27] In addition, the presence of intra-alveolar hemorrhage may suggest virus-associated hemophagocytic syndrome.[23]

Table 3 - Semiquantitative analysis of electron microscopy.

	Patients				
	Case 1	Case 2	Case 3	Case 4	Case 5
Cytoplasmic swelling	2.5 (2–3)	2 (2–2)	4 (4–4)	3 (3–3)	4 (4–4)
Degenerative changes	2.5 (2–3)	2 (1–3)	4 (4–4)	2.5 (1–4)	3 (3–3)
Sloughing of necrotizing AECI + AECII	3 (2–4)	2.5 (2–3)	4 (4–4)	2.5 (1–4)	3 (2–4)
Denudation of the epithelial basement membrane	2.5 (2–3)	2 (2–2)	3 (3–3)	2.5 (1–4)	4 (4–4)
Hyaline membranes	2 (1–3)	1.5 (1–2)	2 (2–2)	2 (1–3)	1.5 (1–2)
Alveolar septal collapse	2 (1–3)	2 (2–2)	3 (3–3)	2 (1–3)	4 (4–4)
Tubuloreticular structures	3.0 (2–4)	2.5 (2–3)	2 (2–2)	1.5 (1–2)	2 (1–1)
Cylindrical confronting cisternae	3 (2–4)	2.5 (2–3)	2 (2–2)	2 (1–3)	2 (1–3)
Multinucleated AECII	2 (1–3)	1.5 (1–2)	2 (2–2)	1 (0–2)	1 (1–3)

The lung tissue score was obtained independently by two different investigators. The pathologic findings were graded according to a five-point semiquantitative severity-based scoring system: 0 = normal lung parenchyma; 1 = changes in 1–25%; 2 = 26–50%; 3 = 51–75%; and 4 = 76–100% of the examined tissue.
AECI, II, alveolar epithelial cell type I, II.

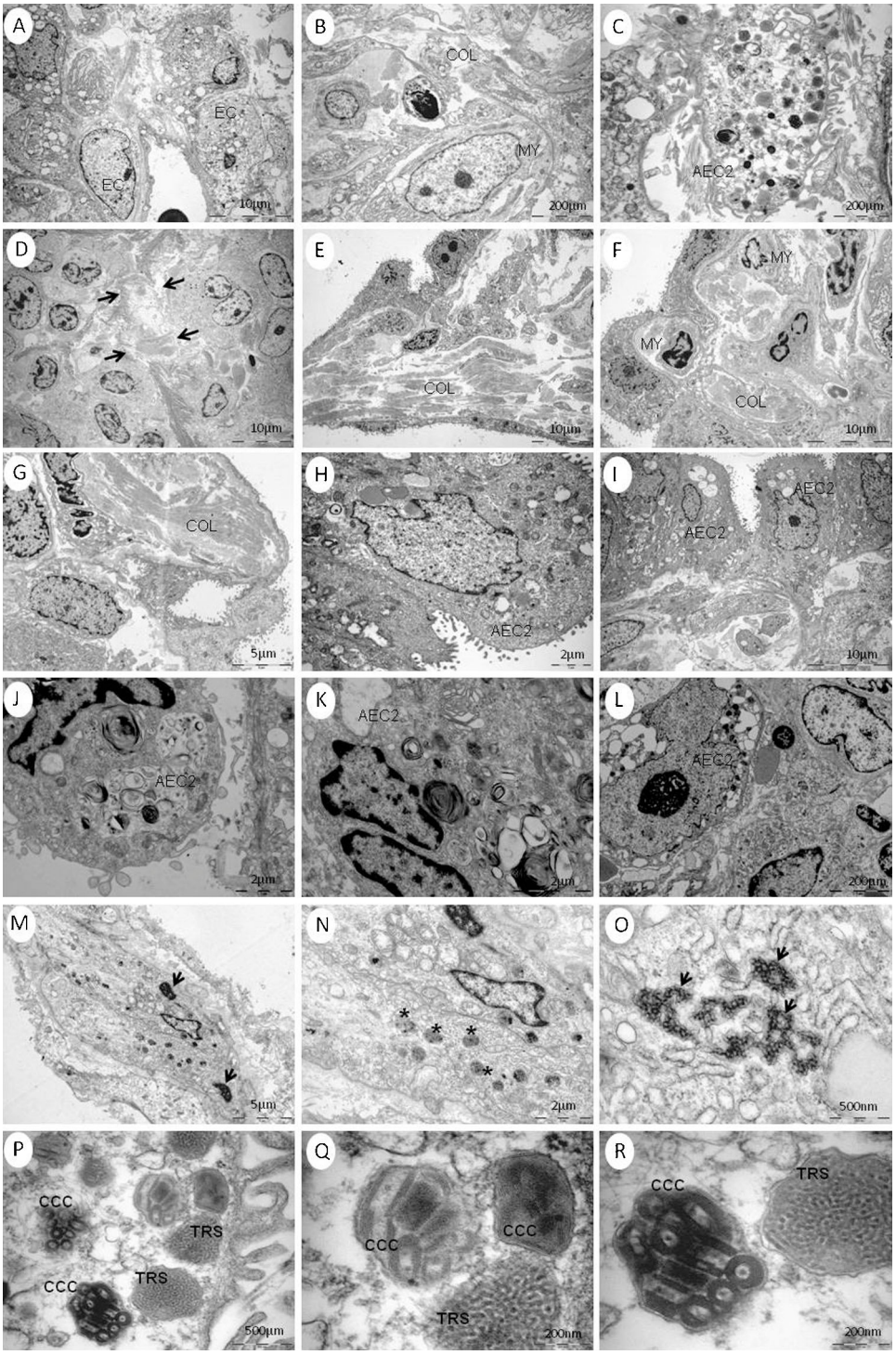

Figure 2 - Ultrastructure sections of lungs from N1H1 patients. Large number of bronchial (EC) and alveolar epithelial cells (AEC2) in apoptosis, note markedly condensed chromatin close to the nuclear membrane (A to C). In panel D, denudation of the epithelial basement membrane and fibrin deposition (arrows). In alveoli, the hyaline membranes appear homogeneous and extend along and partially cover the denuded epithelial basement membranes (D). Regeneration of epithelial cells is shown in panel E to I: note the cells with prominent surface microvilli with decreased or absent lamellar bodies and considerable cytologic atypia. Myofibroblasts (MY) and collagen fibers (COL) were also present (E,F,G). Multinucleated epithelial cells (J,K,L) showing tubuloreticular structures (TRS) and cylindrical confronting cisternae (CCC) representing viral-like particles residuals are shown in M (arrow head), N (star), O (arrow head). TRS showing reticular aggregates of branching membranous tubules located within the cisternae of the endoplasmic reticulum (P,Q,R). Cylindrical confronting cisternae (CCC) showing long cylinders of fused membranous lamellae (M to R), (Uranile and lead citrate).

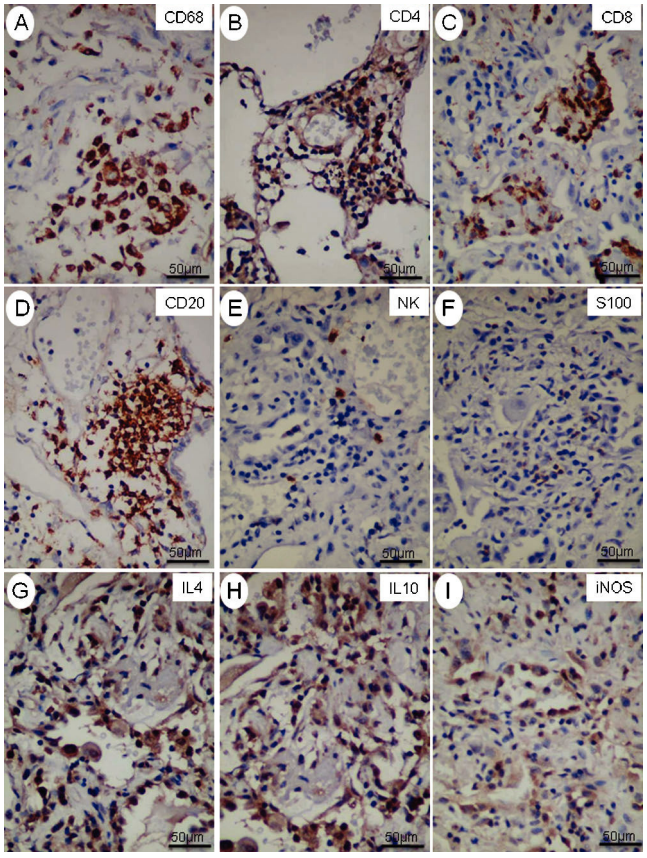

Figure 3 – Immunologic features of lungs from N1H1 patients. Small aggregates of CD68 (A), CD4+ (B), CD8+ (C), CD20+ (D), NK+ (E), and S100+ (F) present around vessels and bronchioles. Note a very strong expression of IL-4 (G), IL-10 (H) and iNOS (I) in macrophages and small mononucleated cells, (Immmunohistochemistry).

In our current series, pulmonary ultrastructural analysis was important to obtain an understanding of the pathophysiology of this new disease. First, we demonstrated apoptosis and necrosis in the bronchiolar epithelium together with viral-like particles, thus suggesting the bronchiolar epithelium as the primary target of the virus infection. Second, we documented the submicroscopic pattern of a clastogenic DAD in S-OIV infection. Third, we found indirect evidence of virus infection in alveolar and bronchiolar epithelial cells represented by the TRS and CCC. These submicroscopic structures were demonstrated ultrastructurally in the lung tissue of all the patients and their presence suggests an inactivation of the virus by oseltamivir treatment or an altered innate immune response of these patients. They appeared mainly in respiratory cells and AECs and have previously been described in a variety of cell types.[28,29] Usually, they occur in endothelial cells and lymphocytes from patients with autoimmune diseases and viral infections.[30] Patients with acquired immunodeficiency syndrome present TRS and CCC in these same cells.[31] The mechanism of TRS and CCC production in vivo is not definitely established. Nevertheless, clinical and experimental studies have shown that the presence of both structures in these diseases is directly associated with the increase of IFNα and IFNβ but not with IFNγ.[29]

One theory to explain the nature and pathogenesis of TRS and CCC suggests that these structures are incomplete viral particles.[30] In our study, these viral-like particles were noted mainly in the respiratory epithelial cells, but not in the other cell types within the lung. These observations reinforce the hypothesis that the primary target cells for S-IOV infection are probably the bronchiolar epithelium. The atypical morphology of the bronchiolar and alveolar epithelial cells was probably related to viral cytopathic effects or reactive changes. In fact, the presence of multinucleated epithelial cells is not exclusive to S-IOV, and is seen in pneumonia caused by the family of Paramyxoviridae, including parainfluenza viruses, measles, mumps, respiratory syncytial virus and, perhaps, metapneumovirus.[31] Although multinucleated cells were seen in our cases, these probably reflect non-specific secondary changes.

We describe a case series of five patients with influenza-like illness with pneumonia and ensuing ARF who underwent OLB with subsequently confirmed diagnosis by RT-PCR testing for S-IOV infections. This report has some limitations. First, this study may not validate the importance of OLB in this population; however, it did provide information about this new disease. Second, it is difficult to compare our findings with those of others because to our knowledge no studies reporting an OLB in patients with S-

Table 4 - Semiquantitative analysis of cell immunophenotypes, cytokine-producing cells, iNOS and caspase.

	Patients				
	Case 1	Case 2	Case 3	Case 4	Case 5
Macrophages	2 (2–2)	2.5 (2–3)	1.5 (0–3)	2.5 (2–3)	1 (1–1)
CD4+ T cells	2 (1–3)	2 (1–3)	1.5 (1–2)	2 (1–3)	1 (1–1)
CD8+ T cells	1 (1–1)	1.5 (1–3)	1 (0–3)	1.5 (0–3)	1 (1–2)
CD20+ B cells	1.5 (1–2)	2 (2–2)	1.5 (1–2)	2 (1–2)	2 (1–3)
Natural killer lymphocytes	1 (1–1)	1 (0–2)	1 (1–1)	1 (1–1)	1 (1–1)
S100+ Dendritic cells	1 (1–1)	1 (1–1)	1 (1–1)	1 (1–1)	0 (0–0)
CD1a+ Dendritic cells	0 (0–0)	1 (0–2)	0 (0–0)	1 (1–1)	0 (0–0)
IFNγ	1 (1–1)	1 (1–1)	0.5 (0–1)	1 (0–2)	1 (1–1)
TNFα	0.5 (0–1)	1 (1–1)	0.5 (0–1)	0.5 (0–1)	0.5 (0–1)
Interleukin 4	3 (2–4)	2.5 (2–3)	4 (4–4)	3 (2–4)	3.5 (3–4)
Interleukin 10	3 (3–3)	3.5 (3–4)	2 (2–2)	3 (3–3)	3 (2–4)
iNOS	3 (2–4)	2.5 (2–3)	4 (4–4)	3 (2–4)	3.5 (3–4)

The lung tissue score was obtained independently by two different investigators. The pathologic findings were graded according to a five-point semiquantitative severity-based scoring system: 0 = normal lung parenchyma; 1 = changes in 1–25%; 2 = 26–50%; 3 = 51–75%; and 4 = 76–100% of the examined tissue.
IFN, interferon; TNFα, tumor necrosis factor α.

IOV have been published. Although there are already many autopsy series with patients with H1N1 that can be used for comparison, the pathological findings at autopsy are modified mainly by the presence of associated co-infections and mechanical ventilation.[32-39]

In summary, we have presented the pulmonary pathology in a confirmed and well-defined series of cases of S-IOV infection associated with ARF. The pathological features, in addition to necrotizing bronchiolitis and DAD, included the presence of multinucleated cells and intra-alveolar fibrin exudates (organizing pneumonia-like lesions). Although each of these features is non-specific, their combined occurrence, together with positive serologic, microbiologic, and immunologic investigations and/or ultrastructural tissue examination enables the diagnosis of S-IOV infection to be confirmed, and is particularly useful in clinically suspicious cases that do not fulfill the WHO criteria or in clinically inapparent cases.

We have shown that viral-like particles can be successfully demonstrated in lung tissue by ultrastructural examination, highlighting the importance of OLB, particularly in those patients without confirmation of the virus. We also showed that bronchioles and epithelium, rather than endothelium, are probably the primary target of infection, and that DAD is the consequence of airways obliteration and dysfunction on innate immunity, suggesting that the treatment should be focused on epithelium repair.

ACKNOWLEDGEMENTS

This study was supported by the following Brazilian agencies: the National Council for Scientific and Technological Development [CNPq]; Foundation for the Support of Research of the State of São Paulo [FAPESP]; and the Laboratories for Medical Research [LIMs], Hospital das Clinicas, University of São Paulo Medical School.

We gratefully acknowledge the excellent technical assistance of Julia Maria L.L. Silvestre, Hélio Correa, Maria Cecília dos Santos Marcondes, Adão Caetano Sobrinho e Carla Pagliari. We are also grateful to Dr. Patrícia Rieken Macedo Rocco, Antônio Carlos Campos Pignatari, Andrea Sette for their help.

REFERENCES

1. Centers for Disease Control and Prevention (CDC). Swine influenza 1. A (H1N1) infection in two children — Southern California, March–April 2009. MMWR Morb Mortal Wkly Rep. 2009;58:400-2.
2. Centers for Disease Control and Prevention (CDC). Update: infections with a swine-origin influenza A (H1N1) virus — United States and other countries, April 28, 2009. MMWR Morb Mortal Wkly Rep. 2009;58:431-3.
3. Centers for Disease Control and Prevention (CDC). Update: swine influenza A (H1N1) infections — California and Texas, April 2009. MMWR Morb Mortal Wkly Rep. 2009;58:435-7.
4. Novel Swine-Origin Influenza A (H1N1) Virus Investigation Team. Emergence of a novel swine-origin influenza A (H1N1) virus in humans. N Engl J Med. 2009;360:2605-15, doi: 10.1056/NEJMoa0903810.
5. World Health Organization - pandemic (H1N1) 2009 - update 77. 2009 December 4. Available from: http://www.who.int/csr/don/2009_10_09/en/
6. Informe epidemiológico Influenza Pandêmica H1N1 (2009), Ed.10, Novembro de 2009. Secretaria de Vigilância em Saúde. Available from: http://portal.saude.gov.br/portal/arquivos/pdf/boletim_influenza_se_47.pdf.
7. Perez-Padilla R, de la Rosa-Zamboni D, Ponce de Leon S, Hernandez M, Quiñones-Falconi F, Bautista E, et al. Pneumonia and respiratory failure from swine-origin influenza a (H1N1) in Mexico. N Engl J Med. 2009;361:680-9, doi: 10.1056/NEJMoa0904252.
8. Chowell G, Bertozzi SM, Colchero MA, Lopez-Gatell H, Alpuche-Aranda C, Hernandez M, et al. Severe respiratory disease concurrent with the circulation of H1N1 influenza. N Engl J Med. 2009;361:674-9, doi: 10.1056/NEJMoa0904023.
9. Barbas CS, Capelozzi VL, Hoelz C, Magaldi RB, de Souza R, Sandeville ML, et al. Impact of open lung biopsy on refractory acute respiratory failure. J Bras Pneumol. 2006;32:418-23.
10. Melo N, Figueiredo S, Morais A, Souto Moura C, Pinho P, Bastos P, et al. Open lung biopsy in patients on mechanical ventilation with suspected diffuse lung disease. Rev Port Pneumol. 2009;15:597-611.
11. Papazian L, Doddoli C, Chetaille B, Gernez Y, Thirion X, Roch A, et al. A contributive result of open-lung biopsy improves survival in acute respiratory distress syndrome patients. Crit Care Med. 2007;35:755–62, doi: 10.1097/01.CCM.0000257325.88144.30.
12. Lim SY, Suh GY, Choi JC, Koh WJ, Lim SY, Han J, et al. Usefulness of open lung biopsy in mechanically ventilated patients with undiagnosed diffuse pulmonary infiltrates: influence of comorbidities and organ dysfunction. Critical Care 2007,11:R93, doi: 10.1186/cc6106.
13. Message SD, Johnston SL. Host defense function of the airway epithelium in health and disease: clinical background. J Leukocyte Biol. 2004; 75:5–17, doi: 10.1189/jlb.0703315.
14. Tamura S, Kurata T. Defense mechanisms against influenza virus infection in the respiratory tract mucosa. Jpn J Infect Dis. 2004; 57:236–47.
15. Murray JF, Matthay MA, Luce JM, Flick MR. An expanded definition of the adult respiratory distress syndrome. Am Rev Respir Dis. 1988;138: 720–3.
16. Riva DR, Oliveira MB, Rzezinski AF, Rangel G, Capelozzi VL, Zin WA, et al. Recruitment maneuver in pulmonary and extrapulmonary experimental acute lung injury. Crit Care Med. 2008;36:1900-8, doi: 10.1097/CCM.0b013e3181760e5d.
17. Passaro CP, Silva PL, Rzezinski AF, Abrantes S, Santiago VR, Nardelli L, et al. Pulmonary lesion induced by low and high positive end-expiratory pressure levels during protective ventilation in experimental acute lung injury. Crit Care Med. 2009;37:1011-7, doi: 10.1097/CCM.0b013e3181962d85.
18. Yamaguchi NH, Lichtenfels AJ, Demarchi LM, da Silva AP, Garippo AL, Alves VF, et al. COX-2, MMP-9, and Noguchi classification provide additional prognostic information about adenocarcinoma of the lung. A study of 117 patients from Brazil. Am J Clin Pathol. 2004;121:78-86, doi: 10.1309/P2CDFGU1U7CLV5YR.
19. Centers for Disease Control and Prevention (CDC). Protocol of real time RT-PCR for swine influenza a (H1N1). 2009 August 24, 2009. Available from: http://www.who.int/csr/resources/publications/swineflu/CDCrealtimeRTPCRprotocol_20090428.pdf.
20. Newman AP, Reisdorf E, Beinemann J, Uyeki TM, Balish A, Shu B, et al. Human case of swine influenza a (H1N1) triple reassortant virus infection, wisconsin. Emerg Infect Dis. 2008;14:1470-2, doi: 10.3201/eid1409.080305.
21. Ng WF, To KF, Lam WW, Ng TK, Lee KC. The comparative pathology of severe acute respiratory syndrome and avian influenza A subtype H5N1 — a review. Hum Pathol. 2006;37:381-90, doi: 10.1016/j.humpath.2006.01.015.
22. Deng R, Lu M, Korteweg C, Gao Z, McNutt MA, Ye J, et al. Distinctly different expression of cytokines and chemokines in the lungs of two H5N1 avian influenza patients. J Pathol. 2008;216:328-36, doi: 10.1002/path.2417.
23. Zheng Y, Yang Y, Zhao W, Wang H. Novel swine-origin influenza A (H1N1) virus-associated hemophagocytic syndrome—a first case report. Am J Trop Med Hyg. 2010;82:743-5, doi: 10.4269/ajtmh.2010.09-0666.
24. Mou SS, Nakagawa TA, Riemer EC, McLean TW, Hines MH, Shetty AK. Hemophagocytic lymphohistiocytosis complicating influenza A infection. Pediatrics. 2006;118:e216-9, doi: 10.1542/peds.2005-1861.
25. Kim B, Ahn KK, Ha Y, Lee YH, Kim D, Lim JH, et al. Association of tumor necrosis factor-alpha with fever and pulmonary lesion score in pigs experimentally infected with swine influenza virus subtype H1N2. J Vet Med Sci. 2009;71:611-6, doi: 10.1292/jvms.71.611.
26. Katzenstein AL, Mukhopadhyay S, Myers J. Diagnosis of usual interstitial pneumonia and distinction from other fibrosing interstitial lung diseases. Human Pathol. 2008;39:1275-94, doi: 10.1016/j.humpath.2008.05.009.
27. Pelosi P, D'Onofrio D, Chiumello D, Paolo S, Chiara G, Capelozzi VL, et al. Pulmonary and extrapulmonary acute respiratory distress syndrome are different. Eur Respir J Suppl. 2003;42:48s-56s, doi: 10.1183/09031936.03.00420803.
28. Grimley PM, Scahff Z. Significance of tubuloreticualr inclusions in the pathobiology of human diseases. Pathobiol Ann. 1976;6:221-57.
29. Sidhu GS, Stahl RE, El-Sard W, Cassai ND, Forrester EM, Zolla-Pazner S. The acquired immunodeficiency syndrome: and ultrastructural study. Hum Pathol. 1985;16:377-86, doi: 10.1016/S0046-8177(85)80231-8.
30. Luu J, Bockus D, Remington F, Luu JY, Bean MA, Hammar SP. Tubuloreticular structures and cylindrical confronting cisterae: a review. Hum Pathol. 1989;20:617-27, doi: 10.1016/0046-8177(89)90148-2.
31. Nicholls JM, Poon LL, Lee KC, Ng WF, Lai ST, Leung CY, et al. Lung pathology of fatal severe acute respiratory syndrome. Lancet 2003;361:1773–8, doi: 10.1016/S0140-6736(03)13413-7.
32. Mauad T, Hajjar LA, Callegari GS, da Silva LF, Schout D, Galas FR, et al. Lung pathology in fatal novel human influenza a (H1N1) infection. Am J Respir Crit Care Med. 2010;181:72-9, doi: 10.1164/rccm.200909-1420OC.

33. Harms PW, Schmidt LA, Smith LB, Newton DW, Pletneva MA, Walters LL, et al. Autopsy findings in eight patients with fatal H1N1 influenza. Am J Clin Pathol. 2010;134:27-35, doi: 10.1309/AJCP35KOZSAVNQZW.
34. Shieh WJ, Blau DM, Denison AM, Deleon-Carnes M, Adem P, Bhatnagar J, et al. 2009 pandemic influenza A (H1N1): pathology and pathogenesis of 100 fatal cases in the United States. Am J Pathol. 2010;177:166-75, doi: 10.2353/ajpath.2010.100115.
35. Gilbert CR, Vipul K, Baram M. Novel H1N1 influenza A viral infection complicated by alveolar hemorrhage. Respir Care. 2010;55:623-5.
36. He YX, Gao ZF, Lu M, Sui GJ, Ran GW, Cao B, et al. A histopathological study on influenza A H1N1 infection in humans. Beijing Da Xue Xue Bao. 2010;42:137-9.
37. Mukhopadhyay S, Philip AT, Stoppacher R. Pathologic findings in novel influenza A (H1N1) virus (''swine flu'') infection: contrasting clinical manifestations and lung pathology in two fatal cases.Am J Clin Pathol. 2010;133:380-7, doi: 10.1309/AJCPXY17 SULQKSWK.
38. Centers for Disease Control and Prevention (CDC). Bacterial coinfections in lung tissue specimens from fatal cases of 2009 pandemic influenza A (H1N1) - United States, May-August 2009. MMWR Morb Mortal Wkly Rep. 2009;58:1071-4.
39. Gill JR, Sheng ZM, Ely SF, Guinee DG, Beasley MB, Suh J, et al. Pulmonary pathologic findings of fatal 2009 pandemic influenza A/H1N1 viral infections. Arch Pathol Lab Med. 2010;134:235-43.